Supplementary Material for

Copper Nitrite Reduction by Thiols: Mechanistic Insights into NO Release *en* route to Copper Thiolate Formation

Naorem Jemes Meitei,[a] Yu-Ting Chu,[b] Chien-Hung Li,[a] Rahimeh Eshaghi Malekshah,[a] Wei-Min Ching,[c] Tsung-Ting Shih,[d] Sodio C. N. Hsu[a,e]*

[a]Department of Medicinal and Applied Chemistry, Drug Development and Value Creation Research Centre, Kaohsiung Medical University, Kaohsiung 807378, Taiwan. E-mail: sodiohsu@kmu.edu.tw

[b]International PhD Program for Science, National Sun Yat-Sen University, Kaohsiung 804201, Taiwan

[c]Department of Chemistry, National Kaohsiung Normal University, Kaohsiung 824005, Taiwan

[d]Department of Chemistry, Fu Jen Catholic University, New Taipei City 242062, Taiwan

[e]Department of Medical Research, Kaohsiung Medical University Hospital, Kaohsiung 807378, Taiwan

*Correspondence: Sodio C. N. Hsu, Department of Medicinal and Applied Chemistry, Drug Development and Value Creation Research Centre, Kaohsiung Medical University, Kaohsiung 807378, Taiwan. E-mail address: sodiohsu@kmu.edu.tw

Supporting information:

Characterization of $LCu(NO_2)$

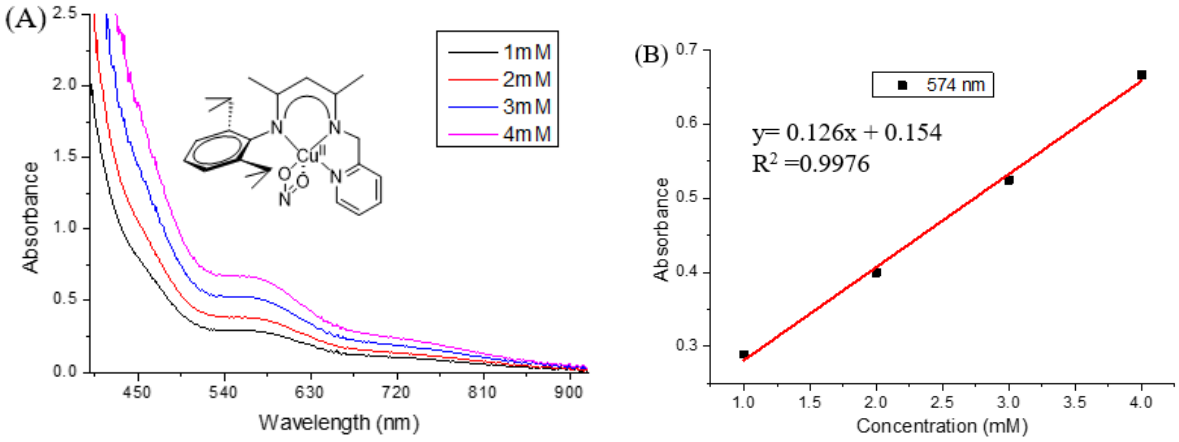

Figure S1: (A) UV-vis spectra of $LCu(NO_2)$ in DCM at 25 °C at different concentrations. (B) Beer's law plot for $LCu(NO_2)$ at 574 nm.

Reaction of $LCu(NO_2)$ with 3 equivalents of 4-*tert*-butyl benzyl thiol (^{t}BuBzSH).

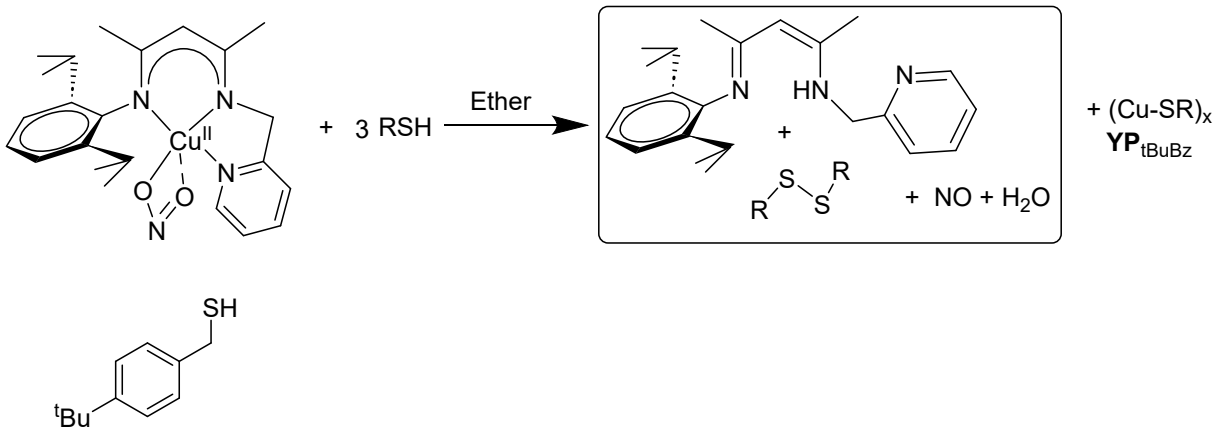

$LCu(NO_2)$ (0.500 g, 1.091 mmol) was dissolved in 10 mL of diethyl ether, and add 4-*tert*-butyl benzyl thiol (^{t}BuBzSH) (0.590 g, 3.27 mmol) was added after mixing with 3 mL of diethyl ether. The color of the reaction mixture slowly changes from dark brown to reddish orange with a clear formation of yellow precipitate and evolution of concomitant gas. The reaction mixture was stirred for 45 min, the reddish solution and yellow precipitate were separated through a glass filter, and dried under a vacuum. ^{1}H NMR analysis on the reddish oily solution in the presence of 1 equivalent of internal standard 1,2,4,5-tetrachlorobenzene provides clear spectra of free β-diketiminate ligand (79%) and *tert*-butyl benzyl disulfide (97%). ^{1}H NMR ($CDCl_3$, 400Hz, 298K): δ 11.32 (bs, 1H, NH), 8.52 (d, 1H, Py1), 7.64 (td, 1H, Py3), 7.36 (d, 4H, *m*-Ar-H), 7.31 (d,1H, Py4), 6.98-7.20 (m, 4H, Ph+Py), 7.19 (d, 4H, *o*-Ar-H), 4.79 (s, 1H, $CH(C{=}N)_2$), 4.59 (s, 2H, CH_2Py), 3.62 (s, 4H, CH_2-Ar), 2.92 (m, 2H, $PhCH(Me)_2$), 1.99 (s, 3H, $CH_3(C{=}N)$, 1.68 (s, 3H, $CH_3(C{=}N)$, 1.34 (s, 18H, ^{t}*Bu*-Ar), 1.18 (d, 6H, $PhCH(Me)_2$), 1.09 (d, 6H, $PhCH(Me)_2$).

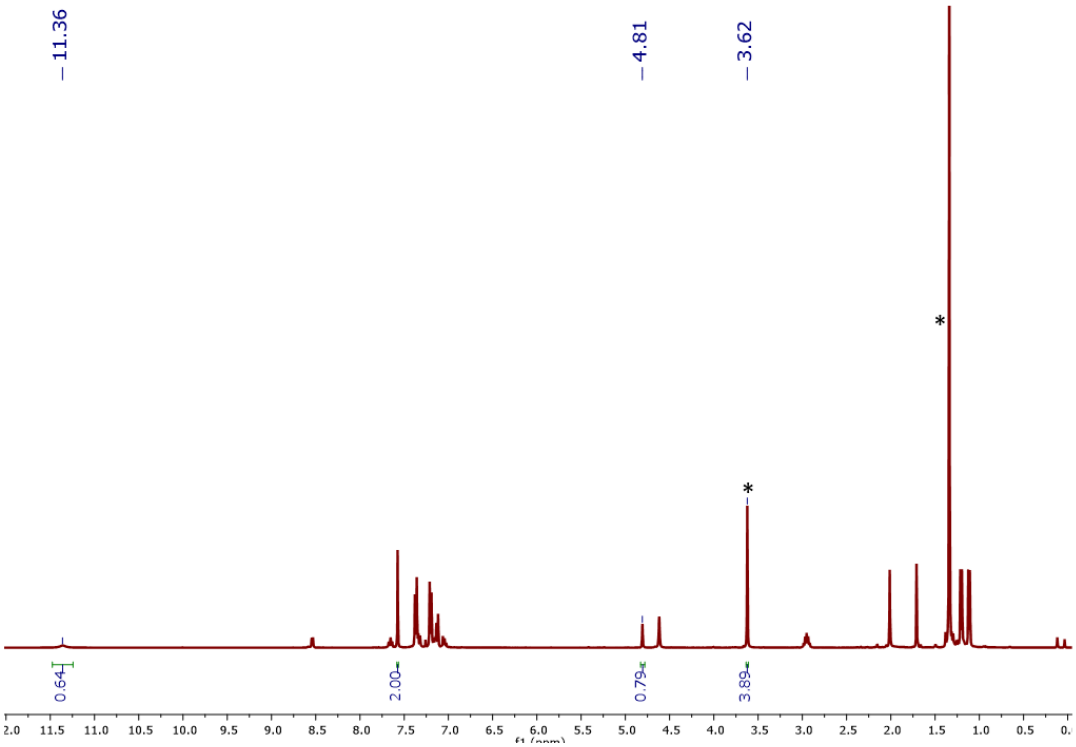

Figure S2. ^{1}H NMR (**400** MHz, $CDCl_3$, 298 K) spectra of crude obtained after the reaction of $LCu(NO_2)$ with 3 equivalents of 4-*tert*-butyl benzyl thiol (^{t}BuBzSH) in the presence of 1 equivalent of 1,2,4,5-tetrachlorobenzene as internal standard, showing a peak at 7.56 ppm, (*) indicates the presence of free dibenzyl disulfide, and the remaining peaks are from the free ligand

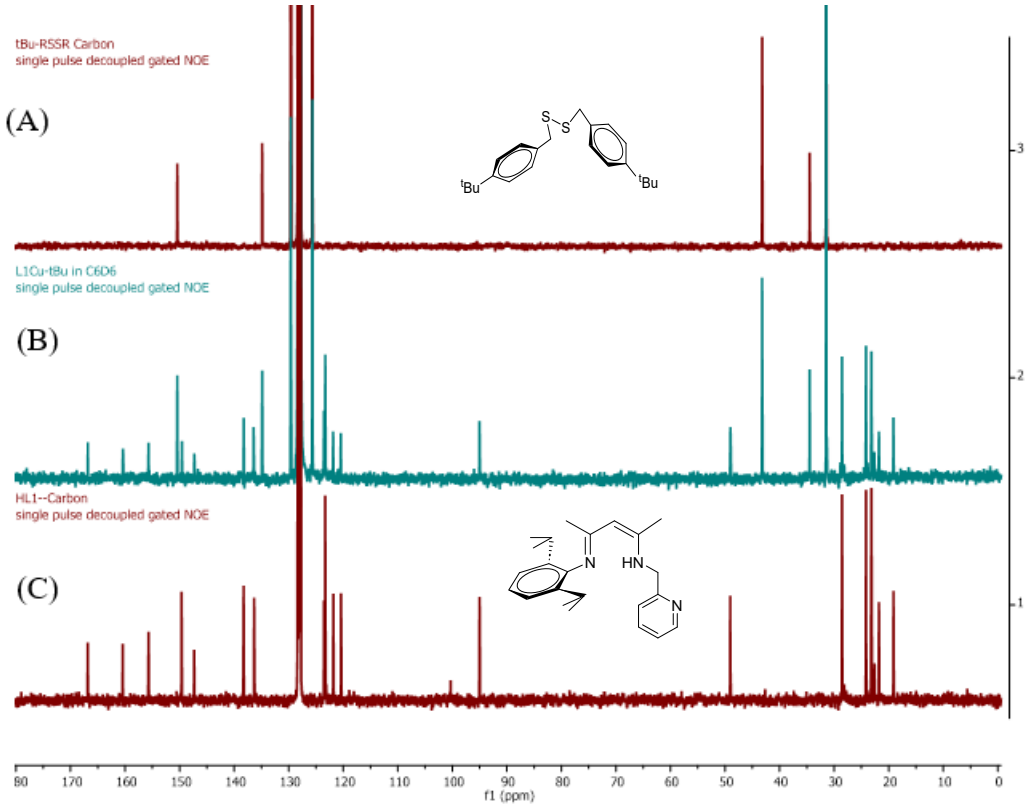

Figure S3: ^{13}C NMR (**400** MHz, C_6D_6, 298 K) comparison spectra of free 4-*tert*-butyl benzyldisulphide (A), crude obtained after the reaction of $LCu(NO_2)$ with 3 equivalents of 4-*tert*-butyl benzyl thiol (^{t}BuBzSH) (B), and free ligand (C). No significant change is observed in this comparison.

The yellow precipitate, after separating the reddish oily filtrate, was washed thoroughly with pentane 3 times with 10 ml and dried under vacuum. FT-IR analysis on the yellow precipitate shows a vibrational peak similar to its corresponding copper thiolate polymer. See Table S1.

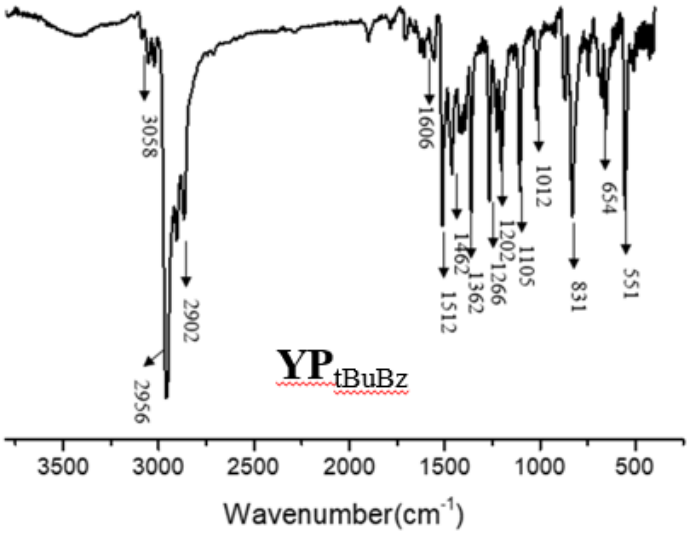

Figure S4. FT-IR (KBr pellet) of the yellow precipitate from the reaction of $LCu(NO_2)$ with 3 equivalents of 4-*tert*-butyl benzyl thiol (^{t}BuBzSH).

Reaction of $LCu(NO_2)$ with 3 equivalents of benzyl thiol (BzSH)

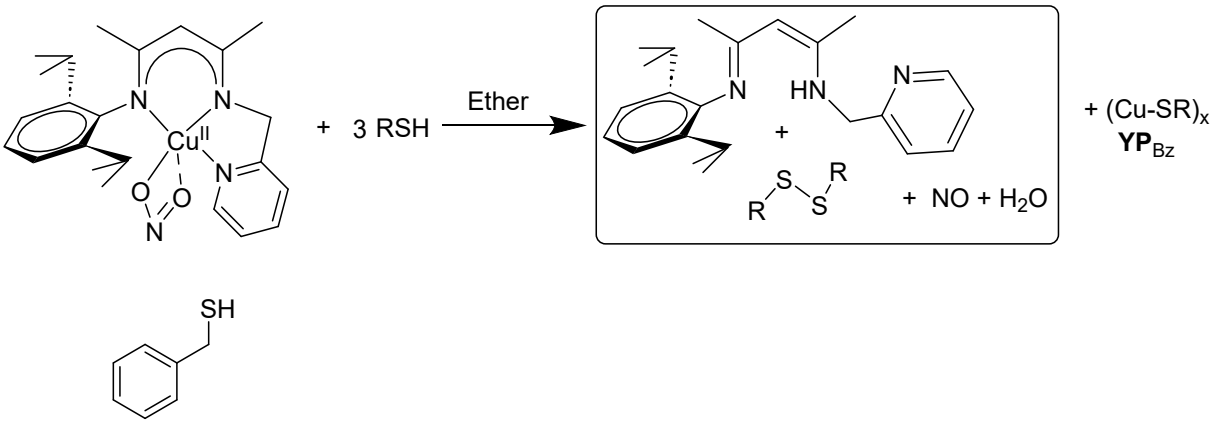

$LCu(NO_2)$ (0.500 g, 1.091 mmol) was dissolved in 10 mL of diethyl ether, and benzyl thiol (BzSH) (0.406g, 3.274 mmol) was added after mixing with 3 mL of diethyl ether. The color of the reaction mixture slowly changes from dark brown to reddish orange with a clear formation of reddish yellow precipitate and evolution of concomitant gas. The reaction mixture was stirred for 45 min, the reddish solution and yellow precipitate were separated through a glass filter, and dried under a vacuum. ^{1}H NMR analysis on the reddish oily solution in the presence of 1 equivalent of internal standard 1,2,4,5-tetrachlorobenzene provides clear spectra of free β-diketiminate ligand (89%) and benzyl disulfide (95%). ^{1}H NMR ($CDCl_3$, 400Hz, 298K): δ 11.32 (bs, 1H, NH), 8.52 (d, 1H, Py1), 7.64 (td, 1H, Py3), 7.26-7.29 (m, 10H, Ar-H),7.31 (d,1H, Py4), 6.98-7.20 (m, 4H, Ph+Py), 4.79 (s, 1H, CH(C=N)2), 4.59 (s, 2H, CH_2Py), 3.60 (s, 4H, CH_2-Ar), 2.92 (m, 2H, PhCH $(Me)_2$), 1.99 (s, 3H, CH_3(C=N), 1.68 (s, 3H, CH_3(C=N), 1.18 (d, 6H, PhCH$(Me)_2$), 1.09 (d, 6H, PhCH$(Me)_2$).

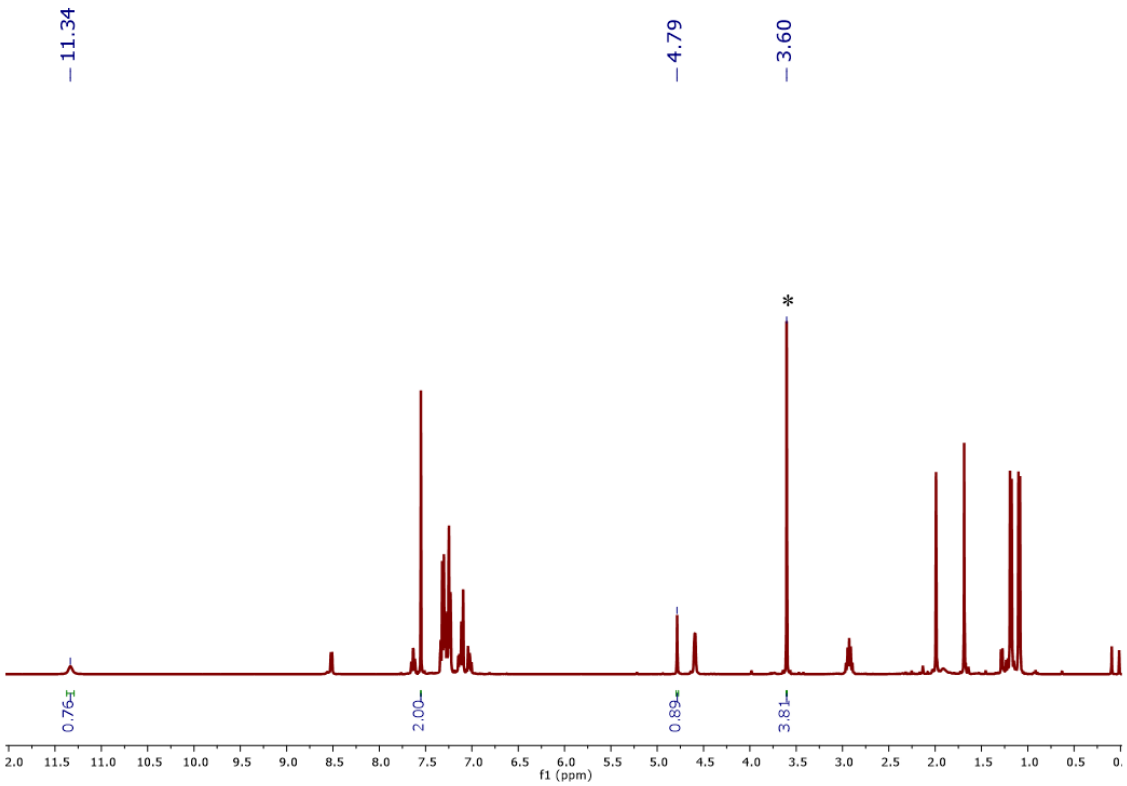

Figure S5. ^{1}H NMR (**400** MHz, $CDCl_3$, 298 K) spectra of crude obtained after the reaction of $LCu(NO_2)$ with 3 equivalents of benzylthiol (BzSH), 1 equivalent of internal standard 1,2,4,5-tetrachlorobenzene, showing a peak at 7.56 ppm, (*) indicates the presence of free dibenzyl disulfide, and the remaining peaks are from the free ligand.

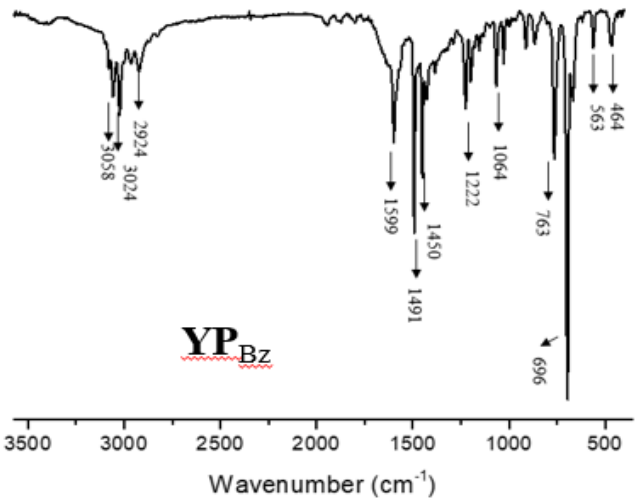

Figure S6. FT-IR (KBr pellet) of the yellow precipitate from the reaction of $LCu(NO_2)$ with 3 equivalents of benzylthiol (BzSH)

Reaction of $LCu(NO_2)$ with 3 equivalents of L-Cysteine (Cys)

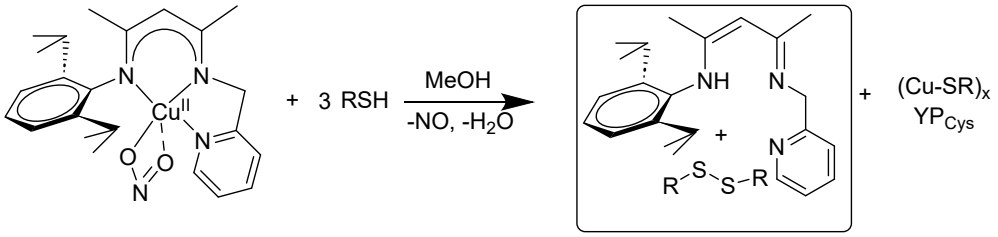

$LCu(NO_2)$ (0.500 g, 1.091 mmol) dissolved in 10 ml of MeOH, and L-Cys (0.396 g, 3.273 mmol) was added after mixing with 5 ml of MeOH. The color of the reaction mixture slowly changes from dark brown to greenish brown with a clear formation of greenish yellow precipitate and evolution of concomitant gas. The reaction mixture was stirred for 45 min, the yellowish-brown solution and greenish yellow precipitate were separated through a glass filter, and dried under a vacuum. ^{1}H NMR analysis of the solution provides a clear spectrum of ligands and free cystine. Due to the difference in the solubility of free ligand and cystine, the ratios are not consistent. ^{1}H NMR (D_2O, 400Hz, 298K): δ 8.62 (bs, 1H, NH), 8.46 (d, 1H, Py1), 8.02 (td, 1H, Py3), 7.64 (d, 1H, Py4), 7.17-7.48 (m, 4H, Ph+Py), 4.42 (s, 2H, CH_2Py), 4.34 (s, 1H, CH(C=N)2), 3.36 (s, 4H, CH_2) 2.76 (m, 2H, PhCH $(Me)_2$), 2.71 (s, 3H, CH_3(C=N), 2.55 (s, 3H, CH_3(C=N), 1.06 (d, 6H, PhCH$(Me)_2$), 0.96 (d, 6H, PhCH$(Me)_2$).

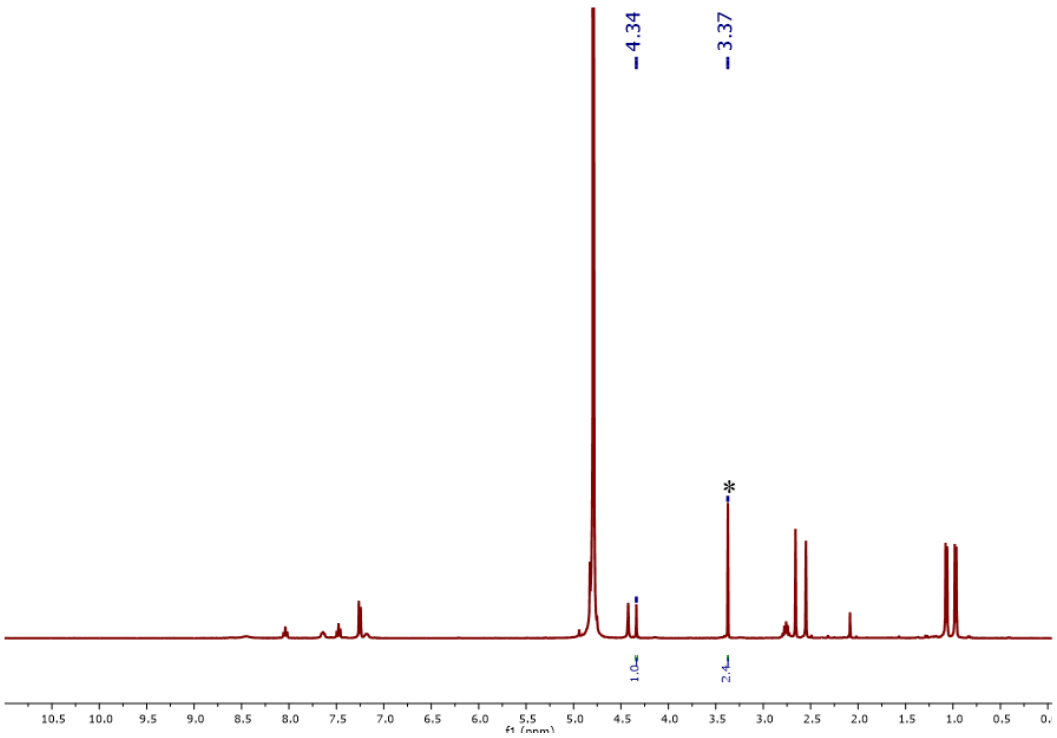

Figure S7. ^{1}H NMR (**400** MHz, D_2O, at 298 K) spectra of crude obtained after the reaction of $LCu(NO_2)$ with 3 equivalents of L-Cysteine (*) indicates the presence of free cystine, and the remaining peaks are from the free ligands.

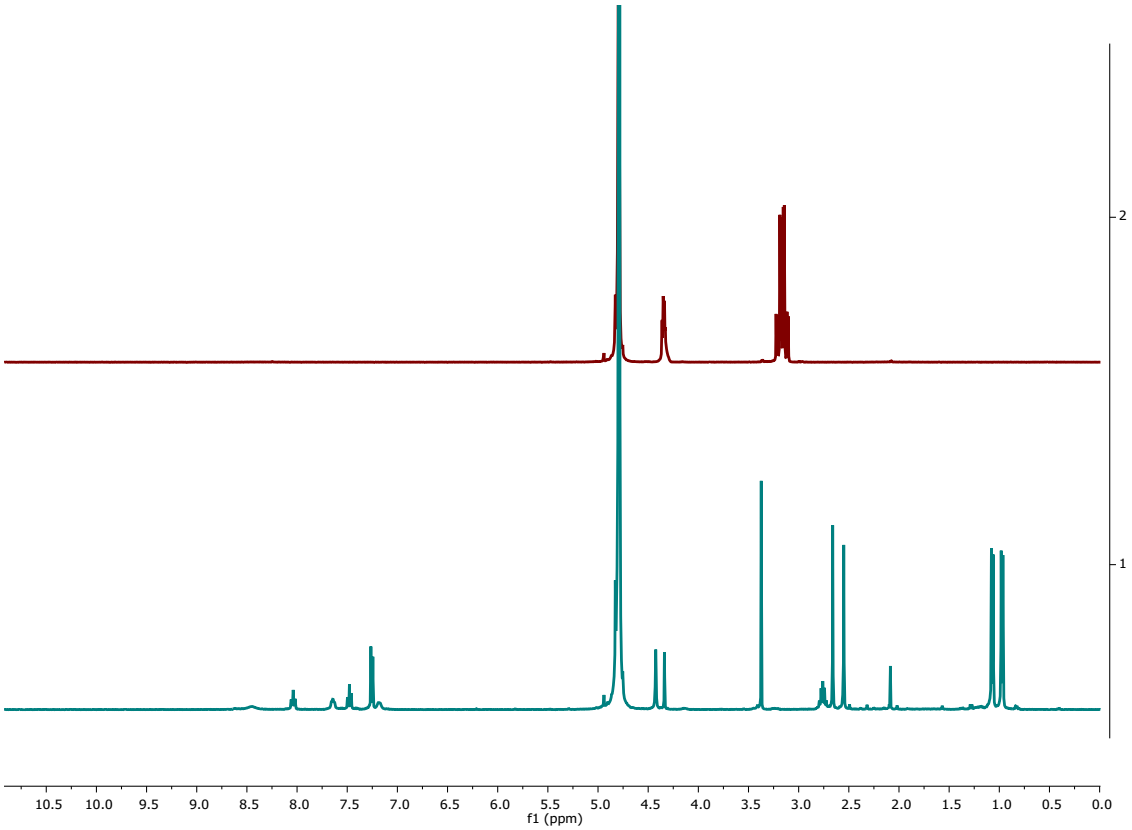

Figure S8. ^{1}H NMR (**400** MHz, D_2O, 298 K) comparison spectra of crude obtained after the reaction of $LCu(NO_2)$ with 3 equivalents of L-Cysteine (Sky Blue) and free L-Cysteine (Red). The shift in the peaks indicates the formation of free cystine

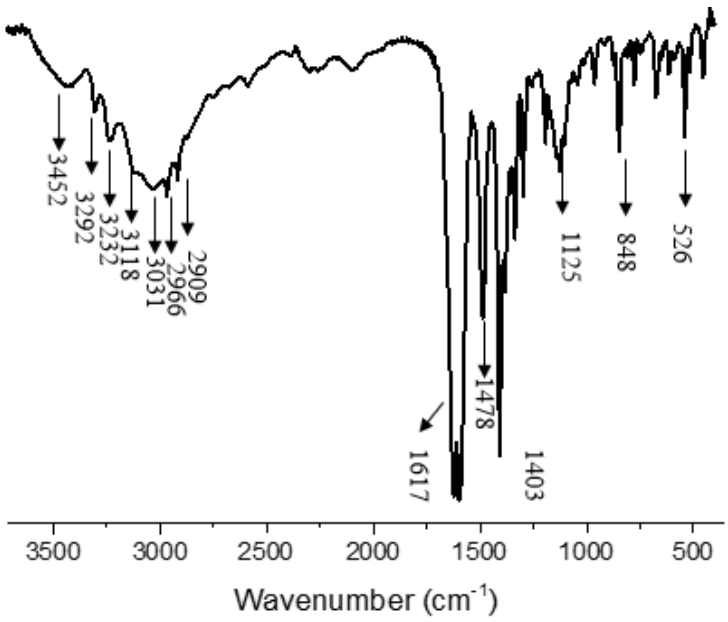

Figure S9. FT-IR (KBr pellet) of the brownish-yellow precipitate from the reaction of $LCu(NO_2)$ with 3 equivalents of L-Cysteine (Cys)

Quantitative NO trapping experiment

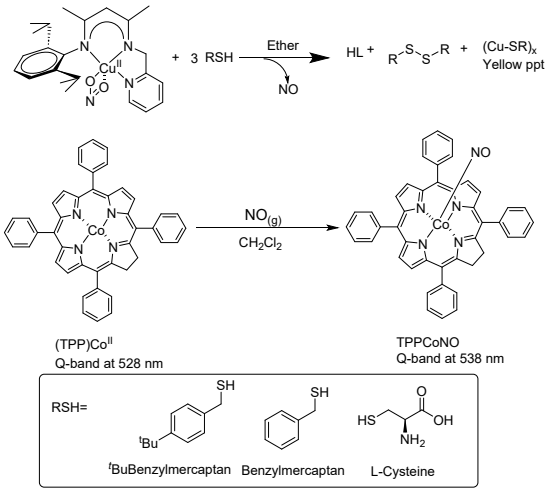

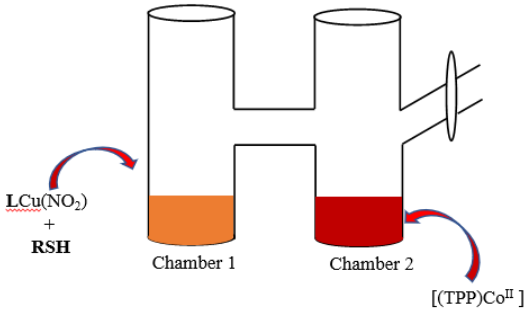

The NO trapping method was employed to investigate the formation of (TPP)CoNO, a key intermediate in the copper-catalyzed nitrite reduction. (TPP)Co was prepared by dissolving (0.043 g, 0.065 mmol) in 2 mL of dichloromethane (DCM). This solution was then added to Chamber 2, providing a controlled environment for the reaction to proceed. In Chamber 1, a solution of the $LCu(NO_2)$ complex was prepared by dissolving (0.030 g, 0.065 mmol) of the complex in 1.5 mL of diethyl ether. This solution provides a source of nitrite ions, which would react with different derivatives of thiols to release NO and trap to form (TPP)CoNO. Three equivalents of 4-*tert*-butyl benzyl thiol (^{t}BuBzSH) (0.035 g, 0.194 mmol) were then mixed with 0.5 mL of diethyl ether and added to Chamber 1, serving as a reducing agent to facilitate the reaction. The mixture was reacted for 30 minutes, during which the formation of (TPP)CoNO was monitored by UV-Vis and NMR spectroscopy. These analytical techniques provided valuable insights for the quantification of NO, allowing us to confirm the successful formation of (TPP)CoNO.

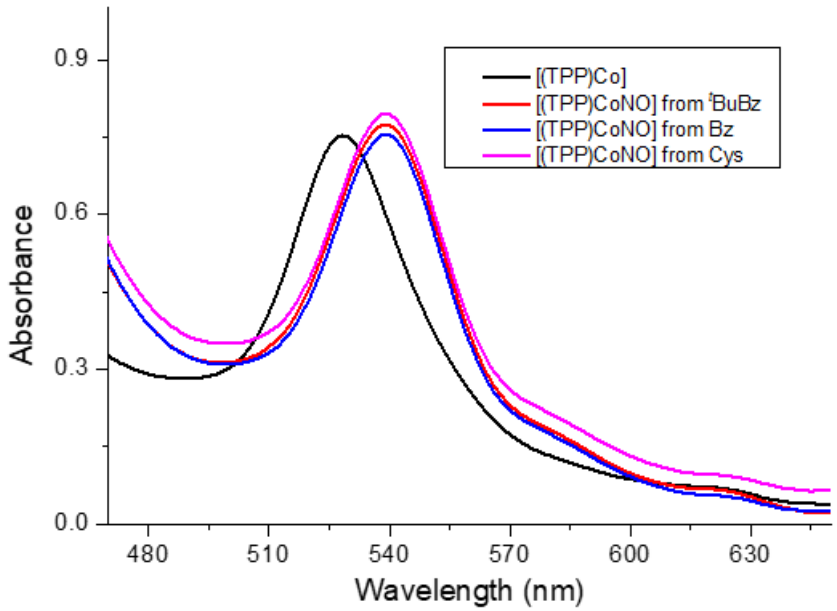

Figure S10. UV-Vis spectra of (TPP)Co (black trace) and (TPP)CoNO (red trace from 4-*tert*-butyl benzyl thiol (ᵗBuBzSH), Blue trace from benzyl thiol (BzSH), and Pink trace from L-Cysteine (Cys) generated by reacting (TPP)Co with NO released from the mixture of LCu(NO_2) and 3 equivalents of RSH. The wavelength shift from 528 nm for (TPP)Co to 530 to 532 nm for (TPP)CoNO is observed. The amount of NO generated was calculated using the calibration curve in Figure S11 and aligns with the reported literature.[1-3]

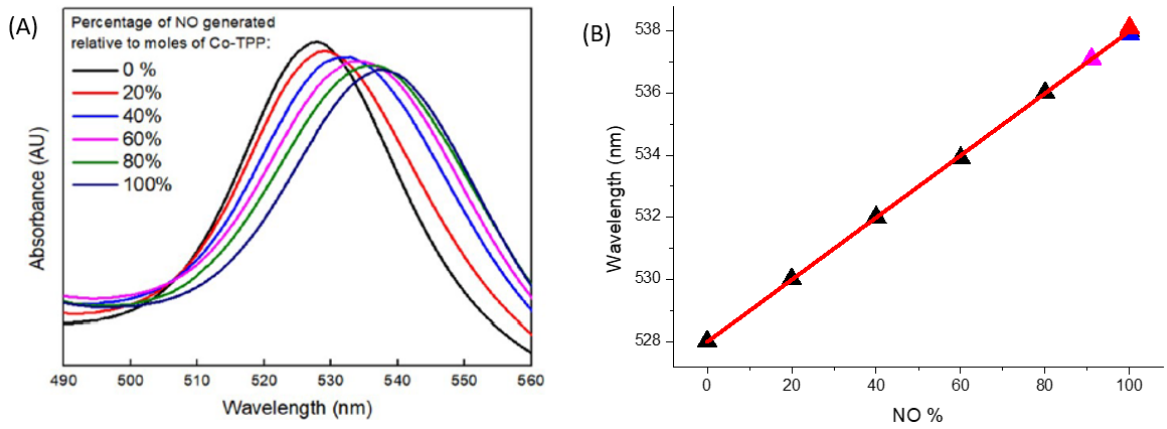

Figure S11. (A) UV-Vis spectra illustrating the red shift in the absorption maximum (λmax) of cobalt(II) tetraphenylporphyrin (TPP)Co upon increasing nitric oxide (NO) complexation. A calibration curve was established by exposing (TPP)Co to defined concentrations of NO in N_2 (160, 320, 480, 640, and 800 ppm). A λ_{max} shift from ~528 nm to ~538 nm was observed with increasing NO concentration. These spectral shifts were plotted against NO levels to construct a calibration curve correlating λ_{max} with NO%. (B) The resulting calibration curve, based on peak maxima, displays a linear relationship between λmax and the percentage of NO complexed. The red 4-*tert*-butyl benzyl thiol (^{t}BuBzSH), blue benzyl thiol (BzSH), and pink L-Cysteine (Cys) points correspond to the NO released from LCu(NO_2) upon treatment with 3 equivalents of the respective thiols.

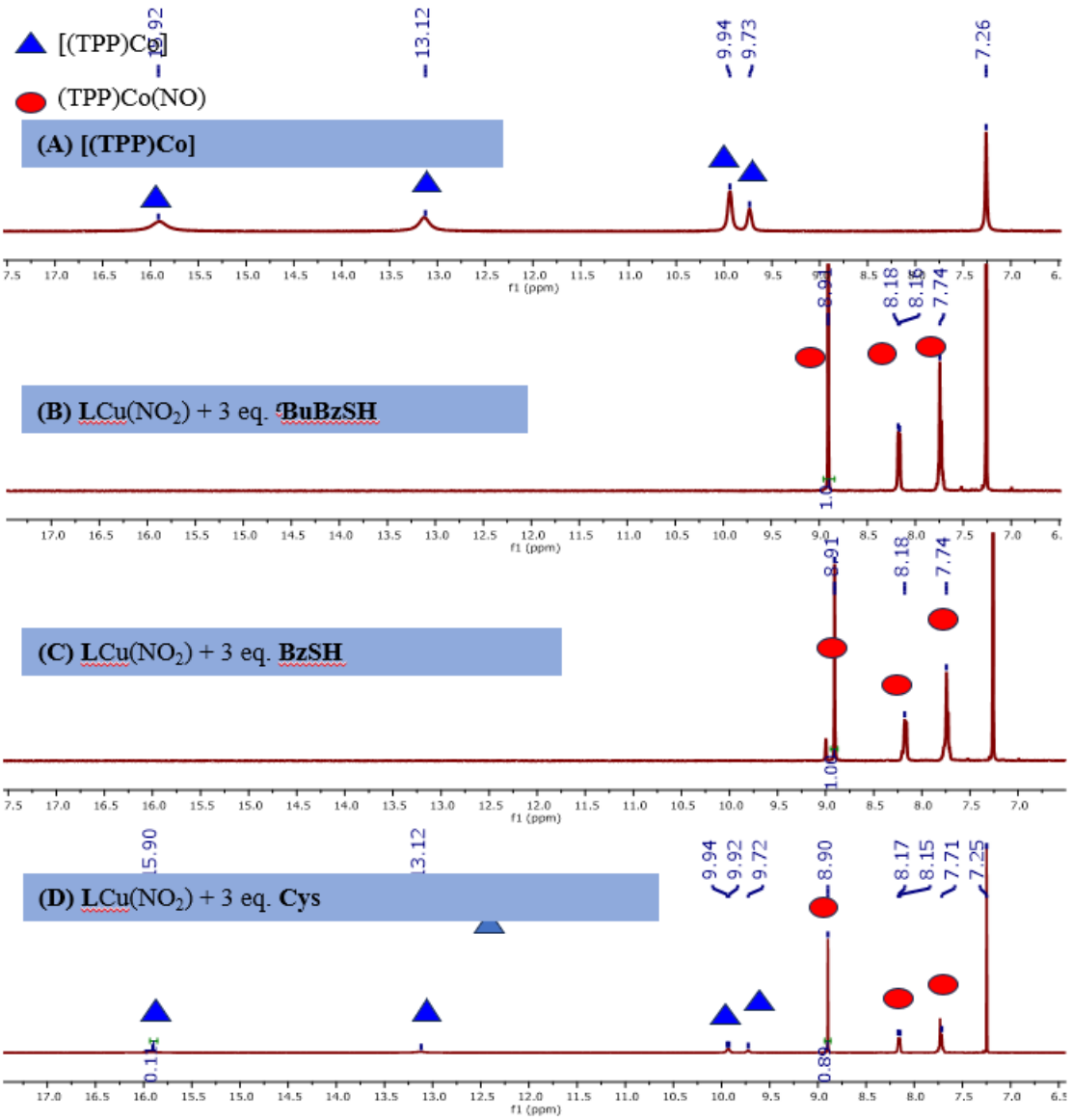

Figure S12. ^{1}H NMR spectra (400 MHz, $CDCl_3$, 298 K) of (TPP)Co recorded after NO trapping experiments involving the reaction of [LCu(NO_2)] with various thiols (RSH). (A) Spectrum of free (TPP)Co, with characteristic signals marked by blue triangles. (B-D) Spectra after reaction with 3 equivalents of (B) 4-*tert*-butyl benzyl thiol (^{t}BuBzSH), (C) benzyl thiol (BzSH), and (D) L-Cysteine (Cys), showing the formation of (TPP)CoNO (highlighted by red circles). The generation of NO was confirmed by the emergence of new resonances corresponding to (TPP)Co(NO), while residual (TPP)Co signals remained visible. Quantitative NO yields were determined by comparing the integrals of (TPP)Co(NO) (δ ≈ 8.91 ppm) and unreacted (TPP)Co (δ ≈ 15.93 ppm).

UV Vis analysis for the reaction of $LCu(NO_2)$ with 1 equiv. of 4-*tert*-butylbenzylthiol (^{t}BuBzSH) at room temperature.

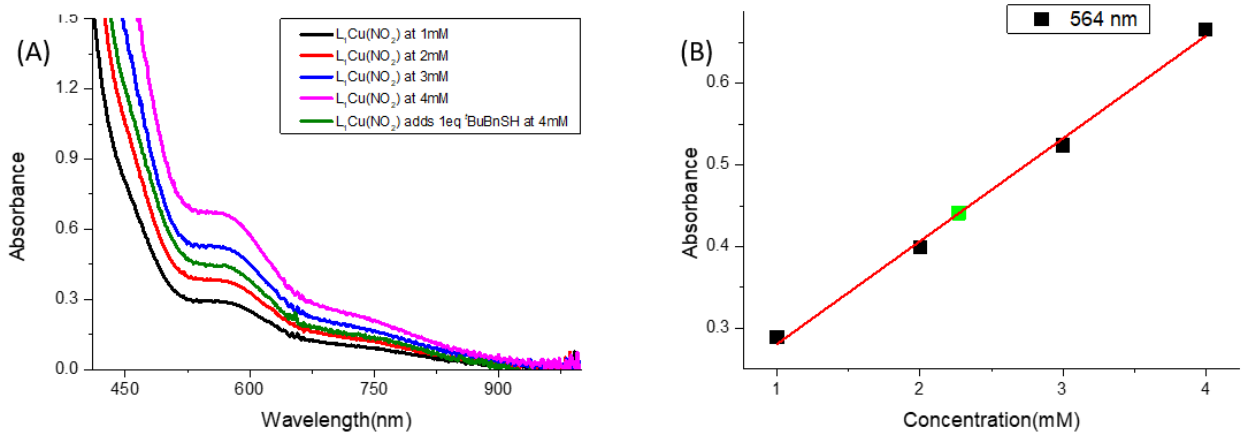

Figure S13. (A) UV-vis spectra of $LCu(NO_2)$ in ether at 25 °C at different concentrations. (B) Beer's law plot for $LCu(NO_2)$ depicts λ_{max}/nm (ε/$M^{-1}cm^{-1}$) = 564 nm along with spectra obtained after adding 1 equivalent of concentrated 4-*tert*-butyl benzyl thiol ^{t}BuBzSH (0.011 mmol) to $LCu(NO_2)$ (0.011 mmol) in 3 mL ether at room temperature, showing approximately 50% unreactivity.

Low-temperature UV Vis analysis for the reaction of LCu(NO_2) with 1 equiv. of 4-*tert*-butyl benzylthiol (^{t}BuBzSH).

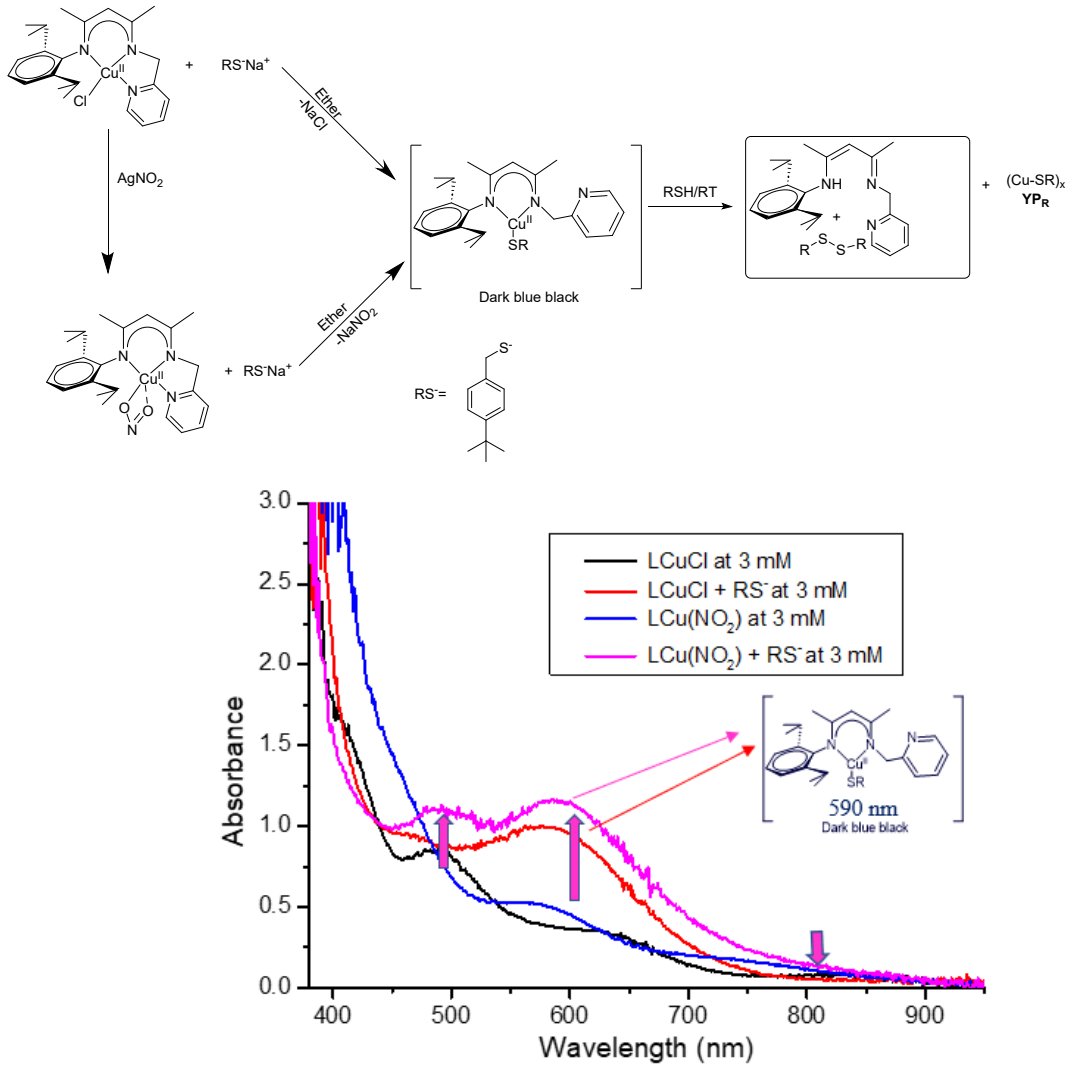

Figure S14. UV-vis spectra of LCu(NO_2) in ether (blue) at -40 °C before and after the addition of an equimolar amount of ^{t}BuBzSH (pink). UV-vis spectra of LCuCl (black) in ether at -40 °C before and after the addition of an equimolar amount of ^{t}BuBzS$^-$ Na$^+$ (red). The above 590 nm blue species is relatively unstable at room temperature.

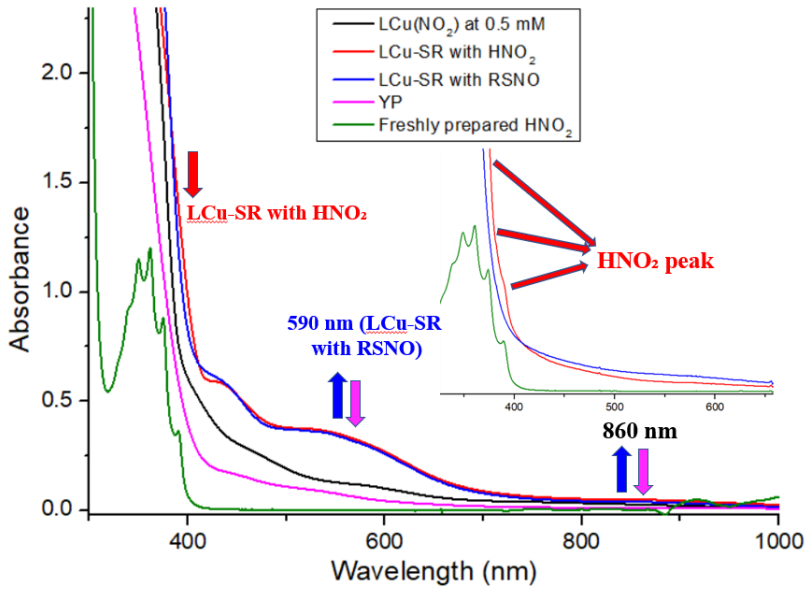

Figure S15. UV-vis spectral changes of $LCu(NO_2)$ (0.5 mM, black trace) in Et_2O at -40 °C upon stepwise addition of ^{t}BuBnSH. Addition of 1 equiv ^{t}BuBnSH generates LCu-SR in the presence of HNO_2 (red trace). Subsequent addition of a second equiv of ^{t}BuBnSH (blue traces) results in decay of the HNO_2 band and growth of features assigned to ^{t}BuBnSNO. Warming the same solution to room temperature after a further equiv of ^{t}BuBnSH affords the Cu(I)-thiolate polymer $\mathbf{YP}_R$ (pink trace). The green trace shows the characteristic HNO_2 spectrum from an independently prepared HNO_2 solution. The inset highlights the HNO_2 band that forms at low concentration upon reaction of $LCu(NO_2)$ with 1 equiv ^{t}BuBnSH in Et_2O at -40 °C (red trace) and decreases after reacting with additional equiv of ^{t}BuBnSH (Blue trace).

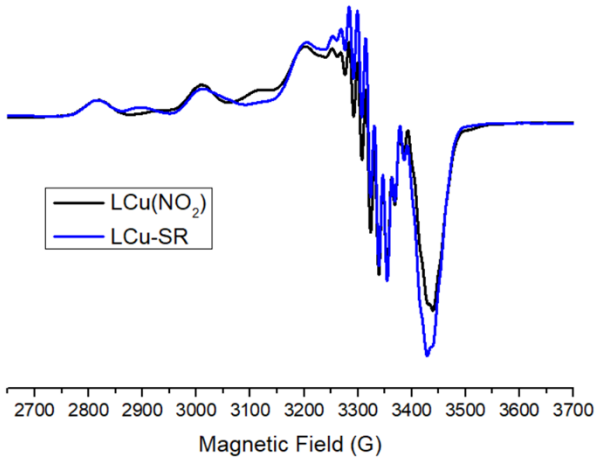

Figure S16. EPR spectrum of LCu(NO_2) (black) and LCu-SR (blue) in DCM at 77 K showing retention of Cu(II) EPR activity upon 4-*tert*-butyl benzyl thiol coordination with a clear color change from brown to blue.

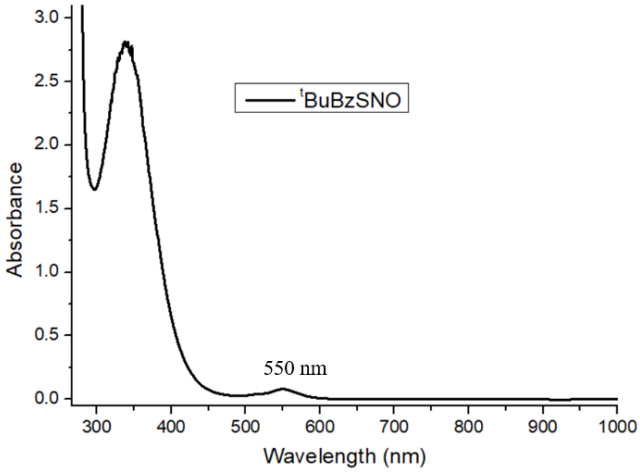

Figure S17. UV-vis absorption spectrum of ^{t}BuBzSNO recorded at room temperature. The S-nitrosothiol was generated *in situ* by rapid reaction of equimolar amount of ^{t}BuBzSH with $NaNO_2$ in aqueous HCl, affording the characteristic RSNO chromophore and its diagnostic electronic absorption features.[4-6]

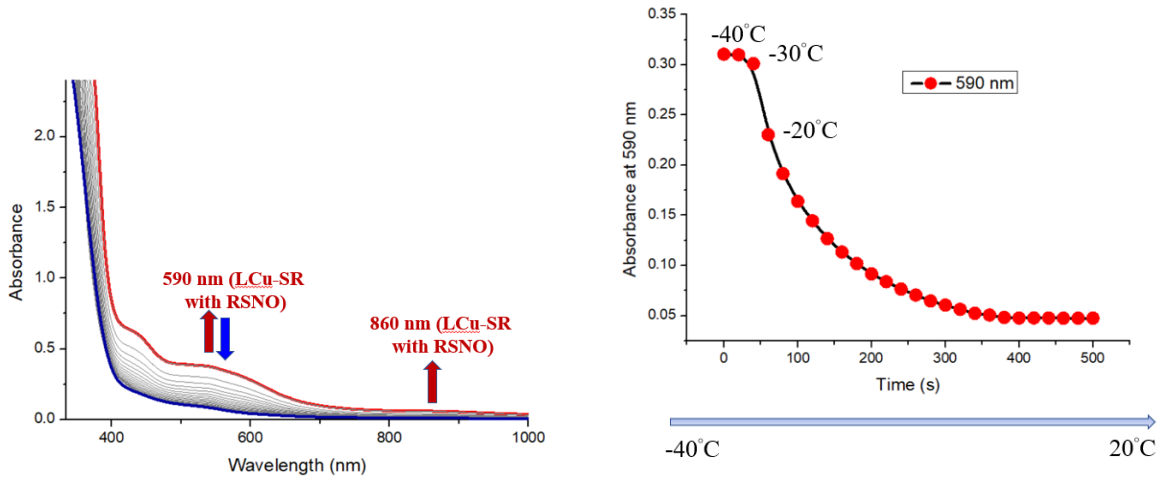

Figure S18. (A) UV-vis spectral changes after addition of ^{t}BuBnSH (3 equiv., concentrated conditions) to LCu(NO_2) (0.5 mM) in Et_2O at 3 mL, showing a transient intermediate with bands at 590 and 860 nm. (B) Upon increasing the temperature from -40 °C to 20 °C, the decay profile of the 590 nm band showing progressive consumption of the transient species.

Analysis of the yellow precipitate by treating with 2,4,5 trimethyl phenyl isocyanide

The yellow precipitate formed from the reaction of $LCu(NO_2)$ with thiols and red oily liquid as free ligand and free disulfide. As the yellow precipitate ($\mathbf{YP}_R$) is insoluble in any solvent, it can't be characterized by NMR. Fortunately, mixing this ($\mathbf{YP}_R$) with 2,4,6-trimethylphenyl isocyanide (CNR) in DCM gives a very clear yellowish-red solution. Investigation of this solution by FT-IR gives a clear blue shift from 2119 cm^{-1} to 2132 cm^{-1}, which can be assigned to the isocyanide bonded to copper.

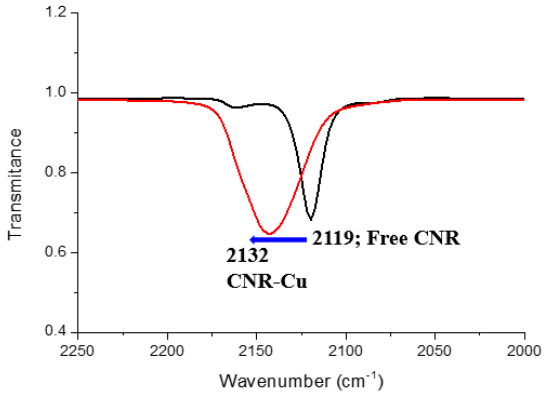

Figure S19. FT-IR spectrum of free trimethyl phenyl isocyanide(black) and $\mathbf{YP}_{tBuBz}$ with 2,4,6-trimethylphenyl isocyanide (red). The blue shift of 2119 cm^{-1} to 2132 cm^{-1} indicates the formation of copper isocyanide adduct. Investigation of this solution by NMR gives a peak that can be assigned to the thiol bonded to copper and a small amount of free disulfide.

Further quantitative ^1H NMR experiments were performed to probe coordination of 2,4,6-trimethylphenyl isocyanide (CNR) to the copper(I) thiolate polymer $\mathbf{YP}_{tBuBz}$ in $CDCl_3$. $\mathbf{YP}_{tBuBz}$ (0.010 g, 0.041 mmol; calculated per Cu-SR unit) was mixed with CNR (0.018 g, 0.121 mmol, 3.0 equiv) in $CDCl_3$ (0.60 mL). The mixture was briefly sonicated to aid dissolution prior to data acquisition. ^1H NMR spectra were recorded for the resulting solution. For quantitative analysis, the benzyl CH_2 protons of the thiolate ligand, expected to be coordinated to copper, appearing at δ 4.01 ppm (2 H) which is different from the free benzyl CH_2 protons of the thiol at δ 3.86 ppm and free disulfide at δ 3.60 ppm, and a well-resolved aromatic resonance of CNR (6 H) were integrated to estimate the CNR:thiolate ratio in solution as seen in **Figure S20**.

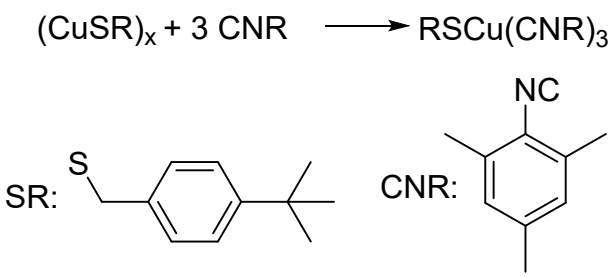

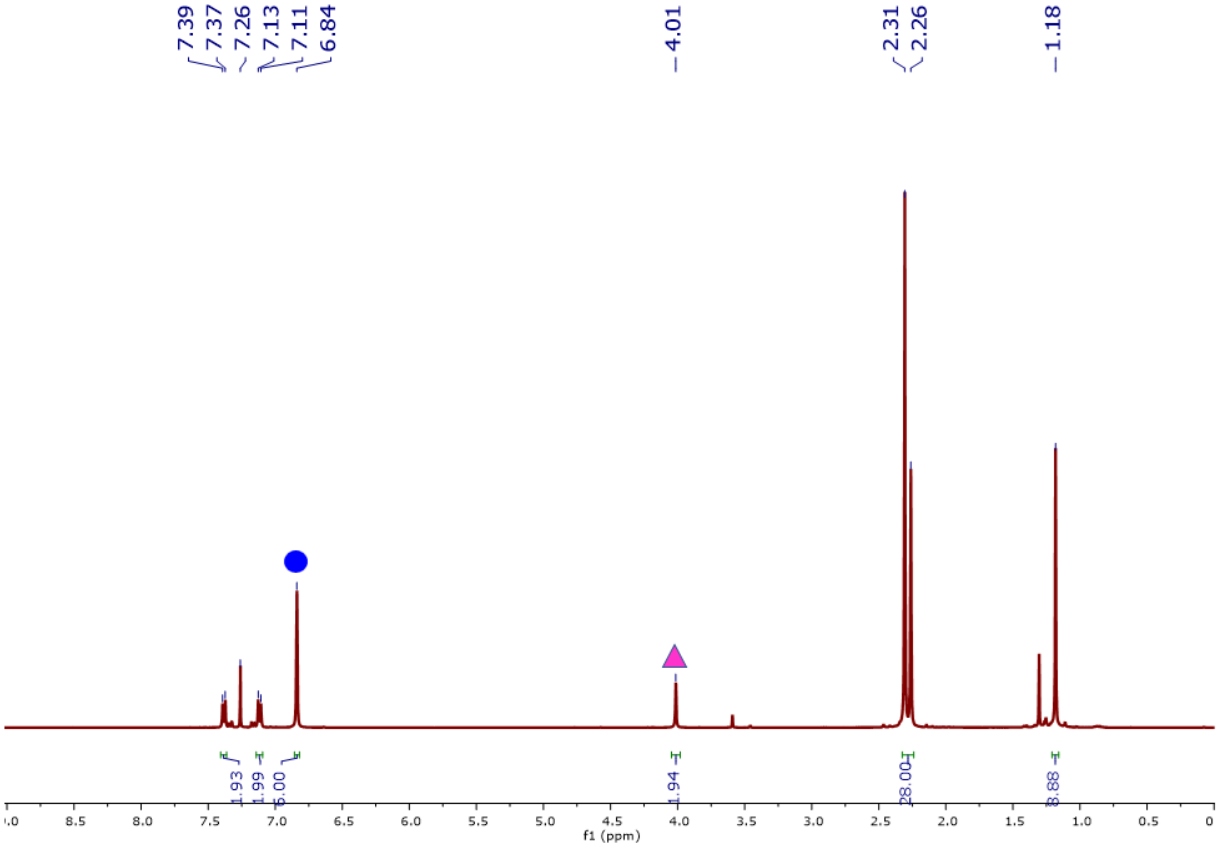

Figure S20: ^{1}H NMR (400 MHz, $CDCl_3$) of the crude product obtained from the reaction of yellow precipitate ($\mathbf{YP}_{tBuBz}$) and trimethyl phenyl isocyanide(CNR) . The peak (▲) comes from the benzyl CH_2 protons of the thiolate ligand, expected to be coordinated to copper (2H), and the peak (●) comes from aromatic resonance of CNR (2H; total 6H)

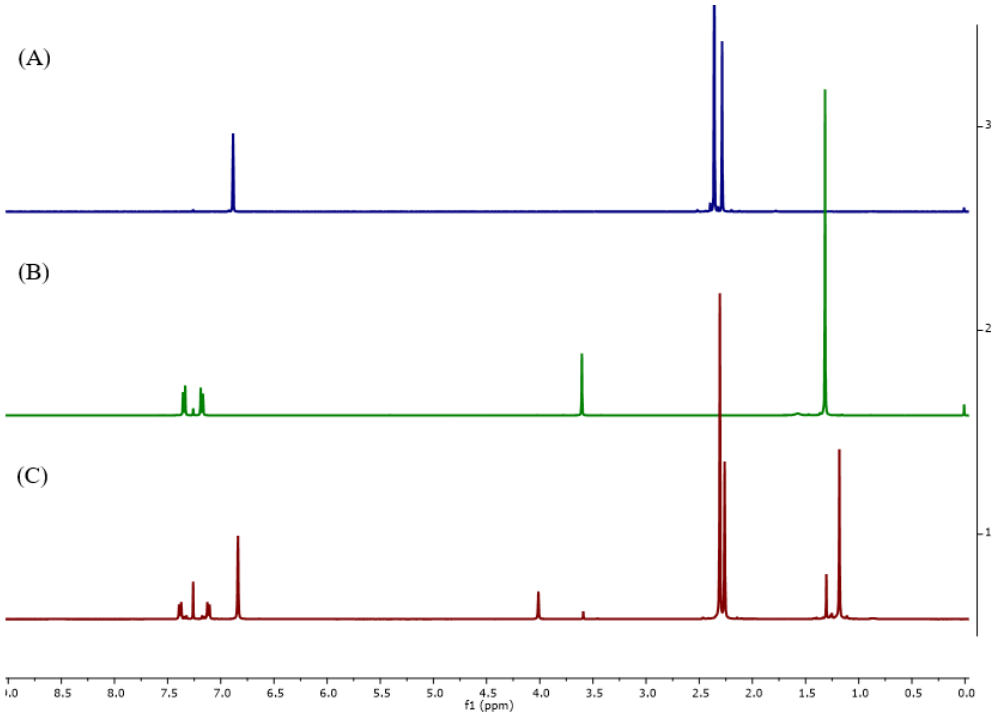

Figure S21: Comparison spectra of ^{1}HNMR (400 MHz, $CDCl_3$) of free 2,4,6-trimethylphenyl isocyanide (A), free disulphide (B), and the crude product obtained from the reaction of yellow precipitate (**YP**$_{tBuBz}$) and 2,4,6-trimethylphenyl isocyanide (C).

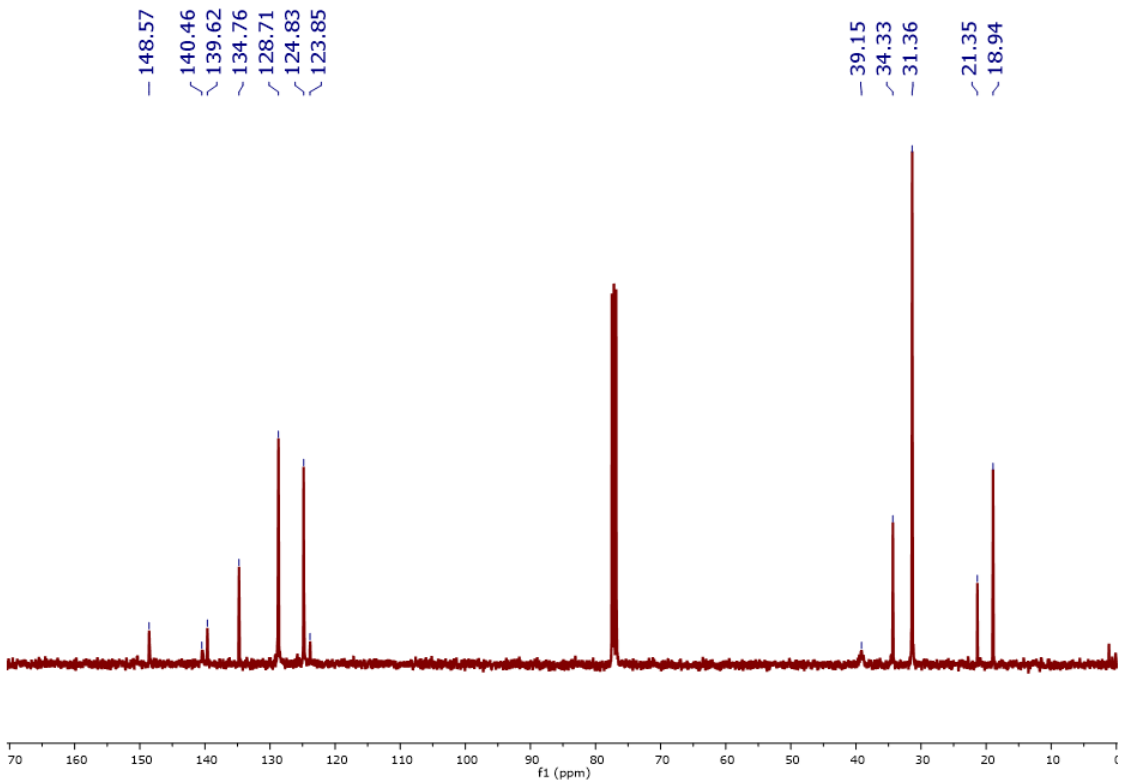

Figure S22: ^{13}C NMR (400 MHz, $CDCl_3$) of the crude product obtained from the reaction of yellow precipitate and trimethyl phenyl isocyanide, assigned according to the roughly expected structure, which is different from free disulphide, 4-*tert*-butyl benzyl thiol (^{t}BuBzSH), and free 2,4,6-trimethylphenyl isocyanide.

Table S1. IR band assignments of Yellow Precipitate ($\mathbf{YP}_R$) from $\mathbf{YP}_{tBuBz}$, $\mathbf{YP}_{Bz}$ and $\mathbf{YP}_{Cys}$ [7, 8]

$\mathbf{YP}_{tBuBz}$	$\mathbf{YP}_{Bz}$	$\mathbf{YP}_{Cys}$	Assignment
---	---	3452	O-H
---	---	3232, 3292	N-H
3058	3058, 3024	---	C-H (Aromatic)
2956, 2902	2924	3118, 3031, 2966, 2909	C-H (Alkyl)
---	---	1617	C=O
---	---	1478, 1125	C-N
----	----	1403	C-O
1606, 1512	1599, 1491		C=C (Aromatic)
1462, 1362	1450		C-H Bending (Alkyl)
1105, 1012	1222, 1064	848	C-H Bending (Aromatic)
654, 555	563, 464	526	C-S

Table S2. Analytical Data: Calculated and Found Elemental Percentages for ($\mathbf{YP}_R$) from $\mathbf{YP}_{tBuBz}$, $\mathbf{YP}_{Bz}$ and $\mathbf{YP}_{Cys}$

$\mathbf{YP}_R$	Assignment	C (%)	H (%)	N (%)	S (%)	Cu-thiolate (%)	Cu_2S (%)
$\mathbf{YP}_{tBuBz}$	$C_{11}H_{15}CuS$	54.41	6.23	–	13.20	100	0
	Found (Result I)	52.76	6.09	–	12.20	~97	~3
	Found (Result II)	52.70	6.33	–	12.12	~97	~3
$\mathbf{YP}_{Bz}$	C_7H_7CuS	45.02	3.78	–	17.17	100	0
	Found (Result I)	42.41	3.59	–	15.35	~94	~6
	Found (Result II)	42.37	3.62	–	15.45	~94	~6
$\mathbf{YP}_{Cys}$	$C_6H_{12}CuN_2O_4S_2$	23.72	3.98	9.22	21.10	100	0

Elemental Analysis for $\mathbf{YP}_R$

Elemental analysis (EA) was performed for all copper-thiolate materials, and repeated measurements were obtained for each sample (**Table S2**). For $\mathbf{YP}_{tBuBz}$ and $\mathbf{YP}_{Bz}$, the expected compositions were calculated for a polymeric Cu(I)-thiolate framework with a 1:1 Cu:thiolate repeat unit. The experimentally observed C and S contents are systematically slightly lower than the calculated values, while H remains close, which is characteristic of polymeric Cu(I)-thiolates containing trace Cu-rich Cu-S condensed domains. Quantitative fitting of the EA data (**Table S2**) indicates compositions of 97 ± 1% Cu(I)-thiolate with 3 ± 1% Cu_2S for $\mathbf{YP}_{tBuBz}$ and 94 ± 1% Cu(I)-thiolate with 6 ± 1% Cu_2S for $\mathbf{YP}_{Bz}$.

In contrast, $\mathbf{YP}_{Cys}$ shows elemental compositions consistent with a 1:2 Cu-thiolate formulation. XPS exhibits Cu 2p shake-up satellite features, confirming Cu(II); accordingly, the EA data were interpreted using a Cu:S = 1:2 stoichiometry. The nitrogen content closely matches the calculated value for $Cu(Cys)_2$, while the sulfur content is slightly reduced. Fitting of the EA data (**Table S2**) gives 92 ± 3% $Cu(Cys)_2$ with 8 ± 3% Cu_2S.

Overall, the EA results (**Table S2**) support polymeric Cu(I)-thiolate frameworks for $\mathbf{YP}_{tBuBz}$ and $\mathbf{YP}_{Bz}$ and a Cu(II)-bis(cysteinate) formulation for cysteine, with minor Cu_2S-type Cu-rich domains accounting for the observed deviations. These results are consistent with the XPS analysis.

Found (Result I)	26.15	5.06	9.26	18.59	~90-95	~5-10
Found (Result II)	25.84	5.06	9.23	18.38	~90-95	~5-10

Note: Result I and II correspond to repeated EA measurements.

Auger Parameter (α′) Calculations for Copper Complexes

The modified Auger parameter (α′) is calculated by summing the binding energy (BE) of Cu $2p_{3/2}$ and the kinetic energy (KE) of the Cu LMM Auger transition which is similar to those of the reported literature.[9-11] KE is obtained by subtracting the binding energy of the Cu LMM peak from the X-ray photon energy (Al Kα = 1486.7 eV).

YP_{tBuBz}

Cu $2p_{3/2}$ BE = 932.32 eV

Cu LMM BE = 570.64 eV

KE = 1486.7 - 570.64 = 916.06 eV

Auger parameter (α′) = 932.32 + 916.06 = 1848.38 eV

YP_{Bz}

Cu $2p_{3/2}$ BE = 932.82 eV

Cu LMM BE = 570.81 eV

KE = 1486.7 - 570.81 = 916.89 eV

Auger parameter (α′) = 932.82 + 915.89 = 1848.71 eV

YP_{Cys}

Cu $2p_{3/2}$ BE = 933.45 eV

Cu LMM BE = 572.01 eV

KE = 1486.7 - 572.01 = 914.69 eV

Auger parameter (α′) = 933.45 + 914.69 = 1848.14 eV

These findings collectively demonstrate that the **YP_R** is composed of copper and thiols, confirming the formation of a copper(I) thiolate polymer.

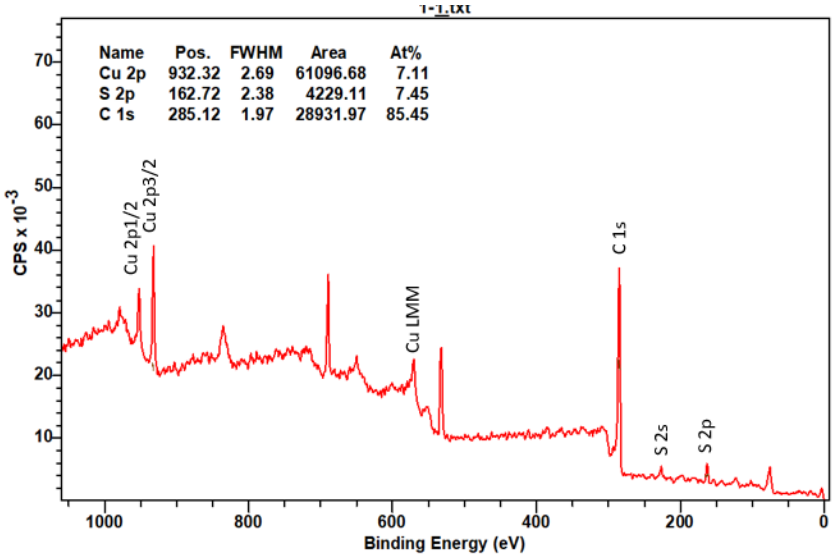

Figure S23. XPS survey spectrum of $\mathbf{YP}_{\mathrm{tBuBz}}$, showing a Cu:S ratio of approximately 1:1.

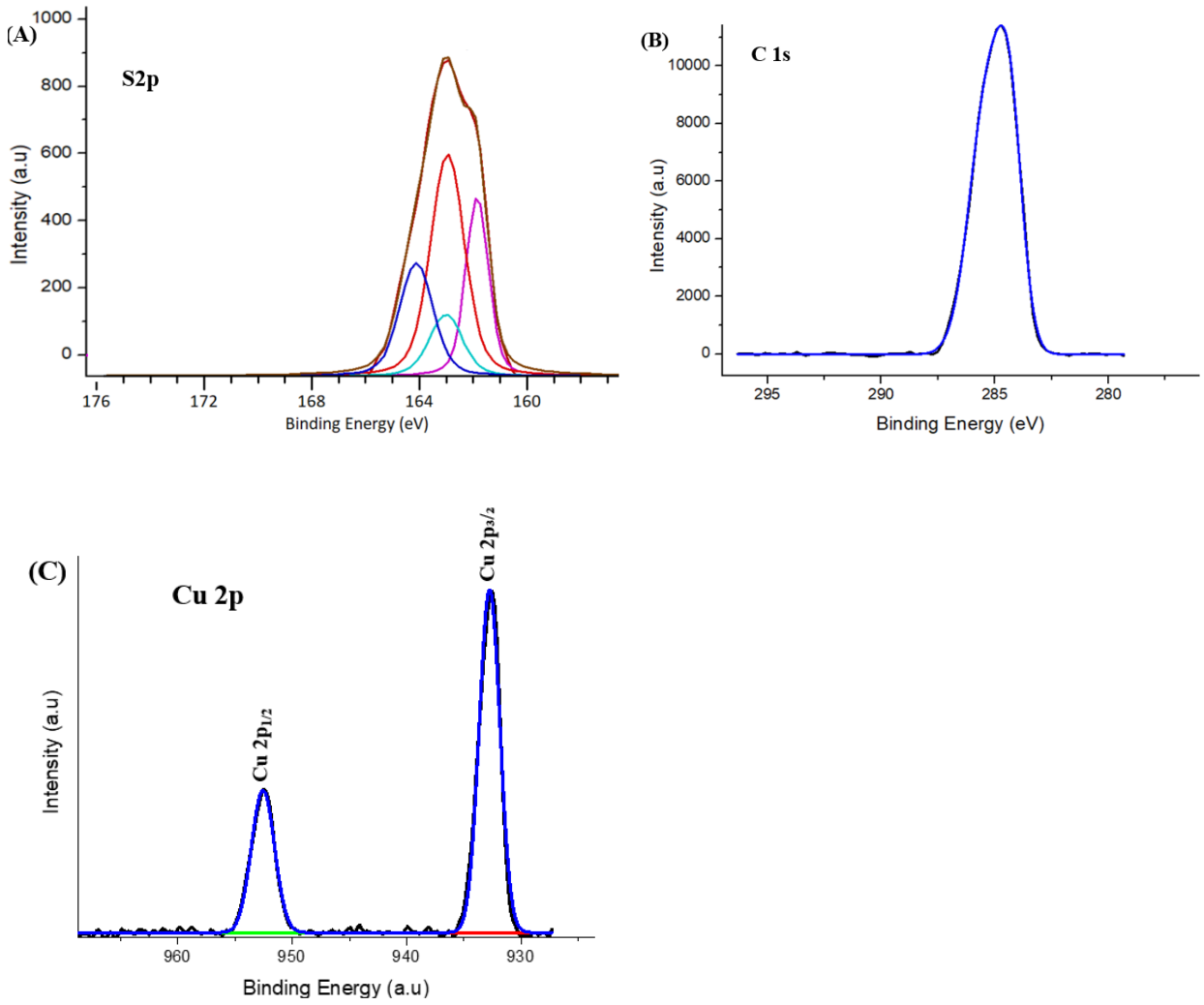

Figure S24. Partial XPS spectrum of $\mathbf{YP}_{tBuBz}$, from the reaction of $LCu(NO_2)$ with 3 equivalents of 4-*tert*-butyl benzyl thiol (^{t}BuBzSH), showing (A) S 2p transitions, (B) C 1S transitions, and (C) Cu 2p transitions.

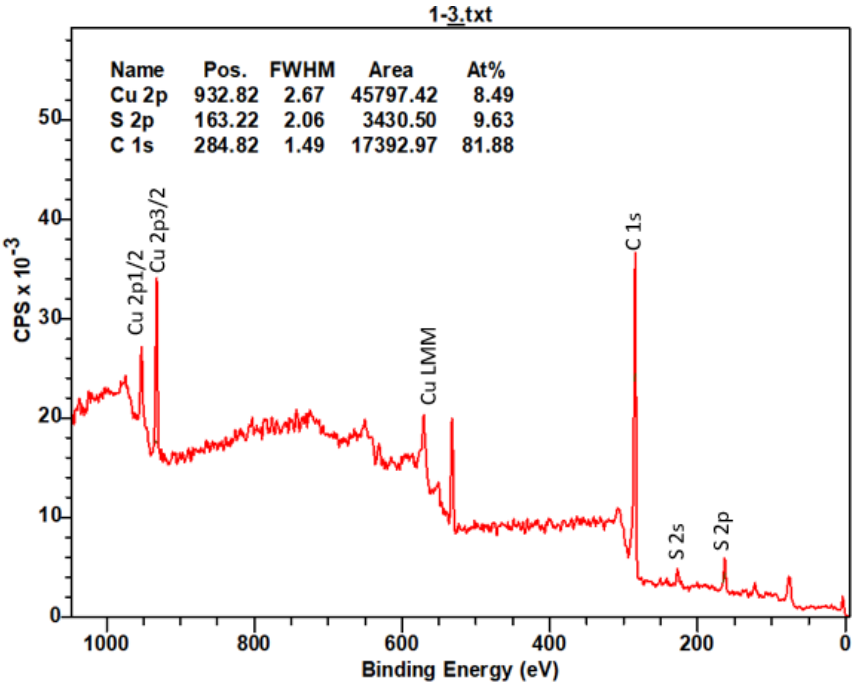

Figure S25. XPS spectrum of $\mathbf{YP}_{Bz}$ indicating a Cu:S ratio of approximately 1:1

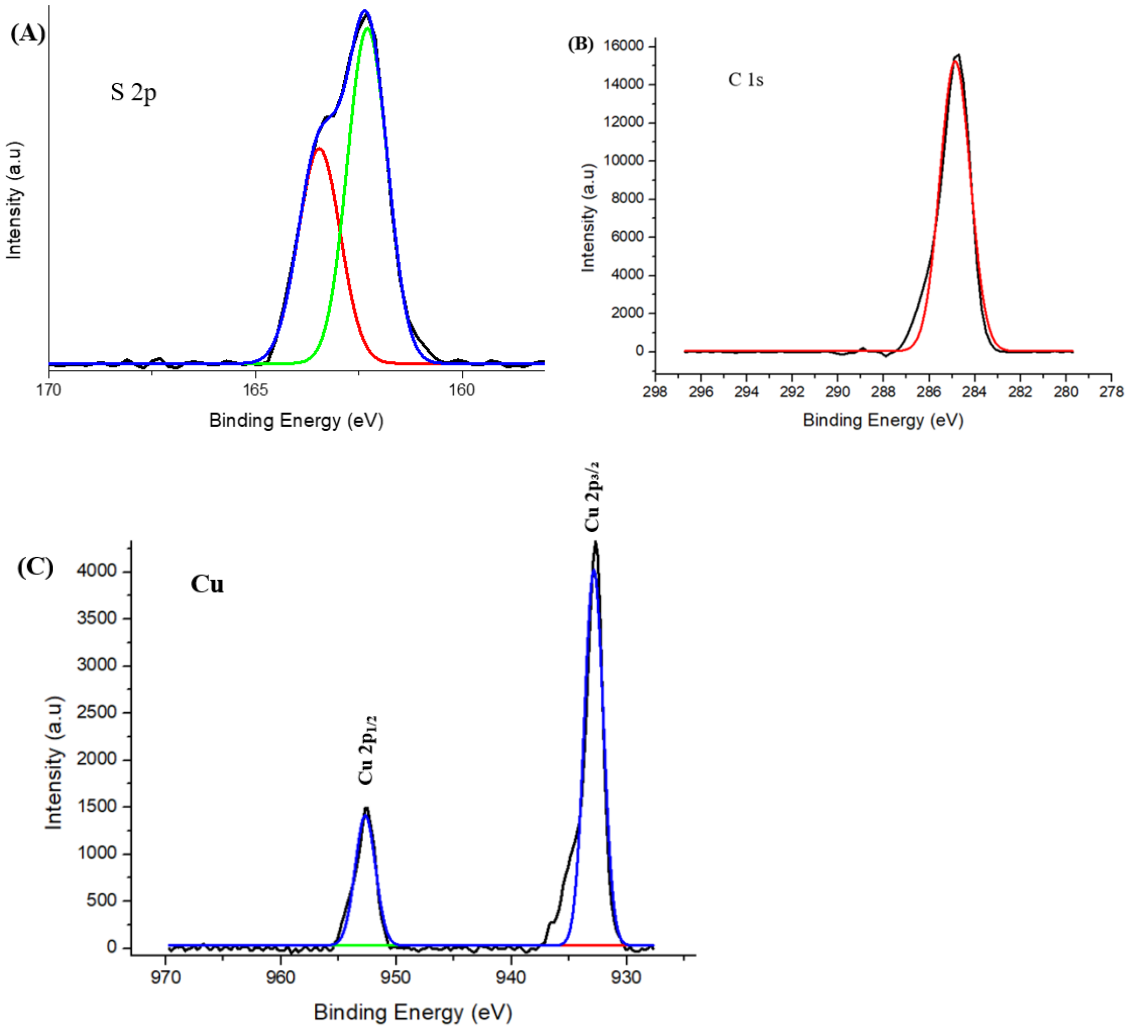

Figure S26. Partial XPS spectrum of $\mathbf{YP}_{Bz}$, from the reaction of $LCu(NO_2)$ with 3 equivalent of benzyl thiol (BzSH), showing (A) S 2p transitions (B) C1s transitions and (C) Cu2p transitions.

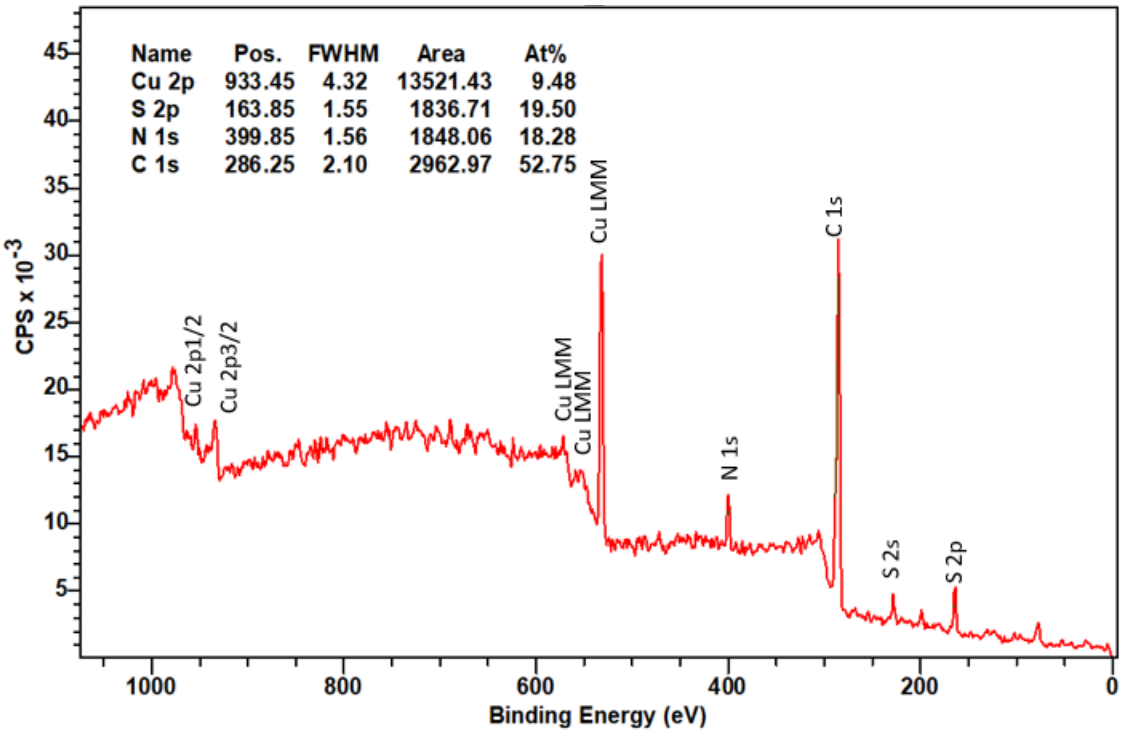

Figure S27. XPS spectrum of $\mathbf{YP}_{Cys}$ indicating a Cu:S ratio of approximately 1:2.

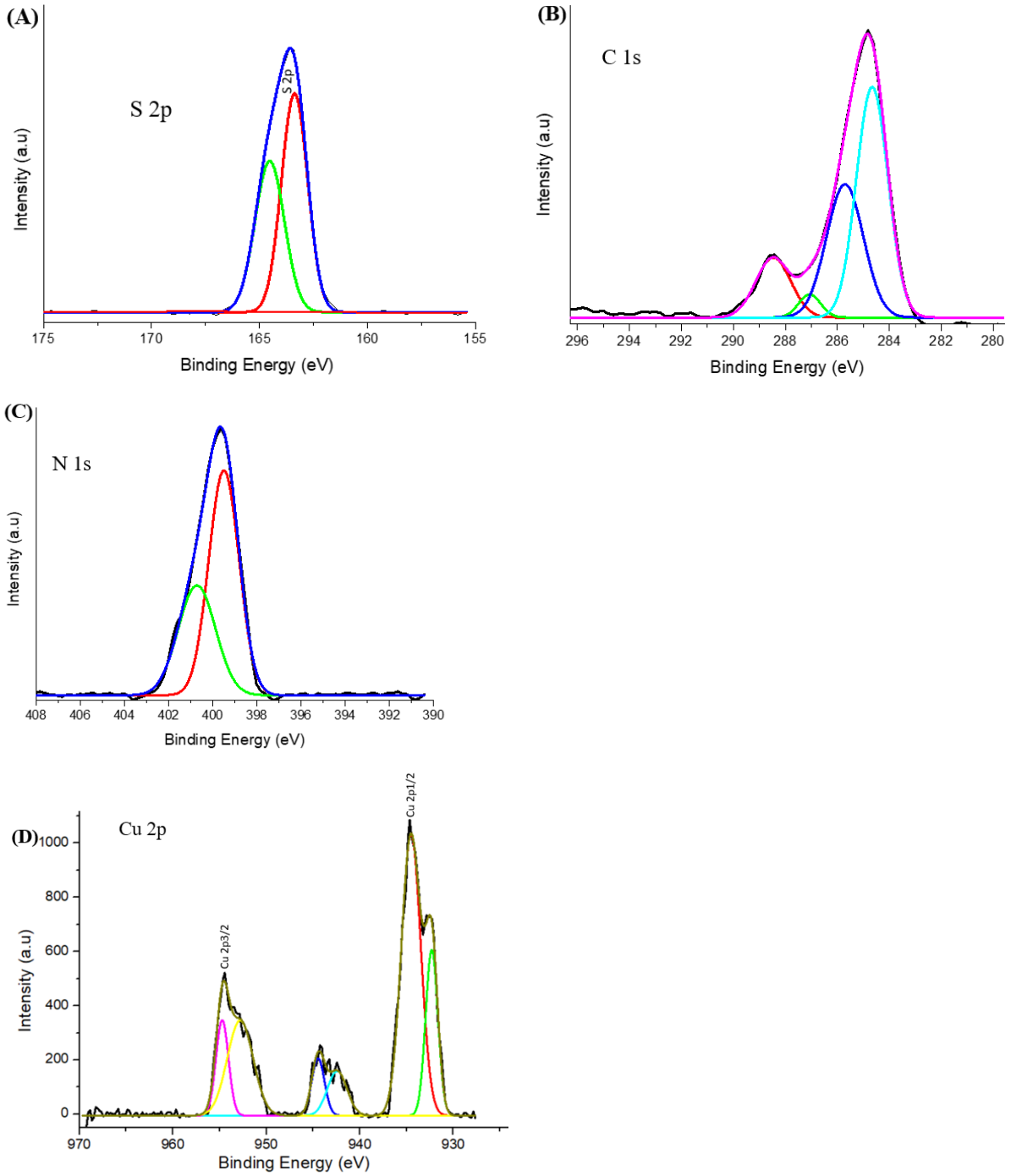

Figure S28. Partial XPS spectrum of $\mathbf{YP}_{Cys}$, from the reaction of $LCu(NO_2)$ with 3 equivalents of Cys, showing (A) S 2p transitions, (B) C 1s transitions, (C) N 1s transitions, and (D) Cu 2p transitions.

Table S3. Expected and experimentally derived copper contents and Cu:thiolate stoichiometries for $\mathbf{YP}_{R}$ materials ($\mathbf{YP}_{tBuBz}$, $\mathbf{YP}_{Bz}$, and $\mathbf{YP}_{Cys}$) determined from ICP-MS Cu contents.

$\mathbf{YP}_{R}$	**Expected Cu:SR ratio**	**Experimental Cu content ($mg \cdot g^{-1}$)**	**Derived Cu:SR ratio**
$\mathbf{YP}_{tBuBz}$	1 : 1	213	~1 : 1.3
$\mathbf{YP}_{Bz}$	1 : 1	268	~1 : 1.4
$\mathbf{YP}_{Cys}$	1 : 2	184.25	~1 : 2.3

Note: ^{t}BuBz: 4-*tert*-butyl benzyl thiol, BzSH: benzyl thiol, Cys: L-cysteine

DFT-D3 Studies

All structures were optimized using DFT-D3 as implemented in Materials Studio 2017 to evaluate two plausible pathways for the formation of Cu(I)-SR, HL, and RSSR species from the parent complex LCu(NO_2). In the first pathway, the reaction proceeds *via* an LCu-OH intermediate (ΔG = +29.779 kcalmol^{-1} and then crosses a transition state (TS; LCu-SR) with an activation barrier of +7.384 kcalmol^{-1}. In the second pathway, the reaction proceeds without formation of the LCu-OH intermediate, reaching the LCu-SR (TS) directly from LCu(NO_2). Notably, the TS lies at a lower endergonic energy than the LCu-OH intermediate, indicating that the direct TS pathway is energetically more favorable than the route involving formation of the intermediate. In addition, the formation of Cu(I)-SR, HL, and RSSR species is thermodynamically favored due to the overall exergonic reaction profile (ΔG = -31.820 kcal mol^{-1}).

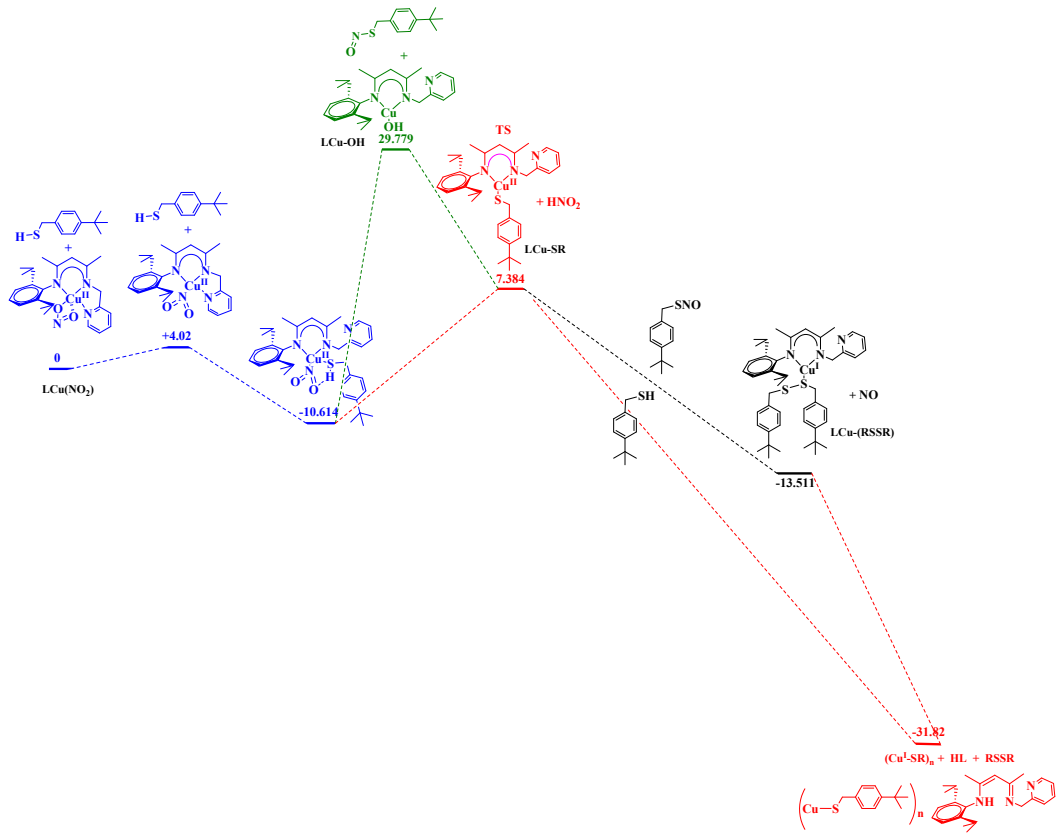

Figure S29. Potential energy profile for the formation of Cu(I)-SR, HL, and RSSR species via two proposed mechanisms derived from DFT-D calculations. The red pathway represents the first and more probable mechanism involving a transition state (TS; LCu-SR), whereas the green pathway corresponds to the second, less favorable mechanism. The black pathway denotes the mechanism previously proposed in the literature; however, our calculations indicate that the red pathway is more favorable based on the Gibbs free energies.

References

1. K. Chand, Y.-C. Chu, T.-W. Wang, C.-L. Kao, Y.-F. Lin, M.-L. Tsai and S. C. Hsu, *Dalton Trans.*, 2022, **51**, 3485-3496.
2. Y.-R. Hsiang, N. J. Meitei, G. E. Henry, S. C. Hsu and Y.-F. Lin, *Dalton Trans.*, 2024, **53**, 18629-18639.
3. Y.-Y. Wang, P.-Y. Chen, N. J. Meitei, Y.-R. Lin, T.-T. Lu, H. D. Nguyen, S. C. Hsu and S.-S. F. Yuan, *J. Inorg. Biochem.*, 2025, **265**, 112833.
4. D. Di Risola, R. Mattioli, G. Mazzoccanti, S. Manetto, M. Trovato, M. Fontana, L. Mosca and A. Francioso, *Separations*, 2022, **9**, 237.
5. T. Sahana, A. K. Valappil, A. S. Amma and S. Kundu, *ACS Org. Inorg. Au.*, 2023, **3**, 246-253.
6. D. L. H. Williams, *Acc. Chem. Res.*, 1999, **32**, 869-876.
7. K. M. Dokken, J. G. Parsons, J. McClure and J. L. Gardea-Torresdey, *Inorg. Chim. Acta*, 2009, **362**, 395-401.
8. M. Wolpert and P. Hellwig, *Spectrochimi. Acta Part A*, 2006, **64**, 987-1001.
9. J. Landoulsi, V. Dupres, C. Méthivier, I. L. Mfiban, P. Cornette, E. Colaço and C.-M. Pradier, *Appl. Surf. Sci.*, 2020, **507**, 145105.
10. A. Tang, S. Qu, K. Li, Y. Hou, F. Teng, J. Cao, Y. Wang and Z. Wang, *Nanotechnology*, 2010, **21**, 285602.
11. Y. Peng, L. Shang, Y. Cao, G. I. Waterhouse, C. Zhou, T. Bian, L.-Z. Wu, C.-H. Tung and T. Zhang, *Chem. Commun.*, 2015, **51**, 12556-12559.